EXPERIMENTAL INVESTIGATION OF THE HEAT TRANSFER IN LAMINAR FORCED CONVECTION FLOW IN A GROOVED CHANNEL

C.V. Herman[1] and F. Mayinger[2]

[1]Universitet u Novom Sadu, Veljka Vlahovića 3, 21 000, Novi Sad, YU
[2]Lehrstuhl A für Thermodynamik, TU München, Arcisstr. 21, 8000 München 2, FRG

ABSTRACT

The subject of the present study is heat transfer in laminar forced convection flow in a grooved channel. In fully developed flow conditions the thermal boundary layer develops in the test section. The test section is a parallel plate duct with one heated wall with four grooves and the opposite plane wall. The aspect ratio of the grooves is a constant value, w:h = 4:1. The method of holographic interferometry is used to visualize the temperature field. In the paper, the heat transfer process in this complex geometry has been analysed in detail. Temperature profiles at different cross sections of the test section and local Nusselt number values along the investigated geometry are presented. It is shown that heat transfer augmentation is due to the increased local heat transfer in the redevelopment region, immediately after the reattachment of the flow.

1. INTRODUCTION

Heat transfer and fluid flow in geometries with backsteps, roughness elements and grooves are important research topics in the heat transfer and fluid mechanics research today. Although a number of theoretical and experimental investigations treating these problems has been published in the literature, only a few of them analyse heat transfer in multiple grooves on a micro scale.

This paper deals with heat transfer in a geometry with four grooves (presented in figure 1) in laminar forced convection flow, with air as the working fluid. This physical situation is frequently encountered in various engineering applications: in the cooling of electronic equipment cavities are formed by the spaces between circuit components on electronic circuit boards, in heat exchangers roughness elements and turbulence promoters are used to improve heat transfer, similar geometries are encountered in nuclear reactor cores, etc.

There has been a significant number of studies, devoted to this class of physical problem, published in the literature. The references in this publication are selected for their relevance for the specific situation treated in the

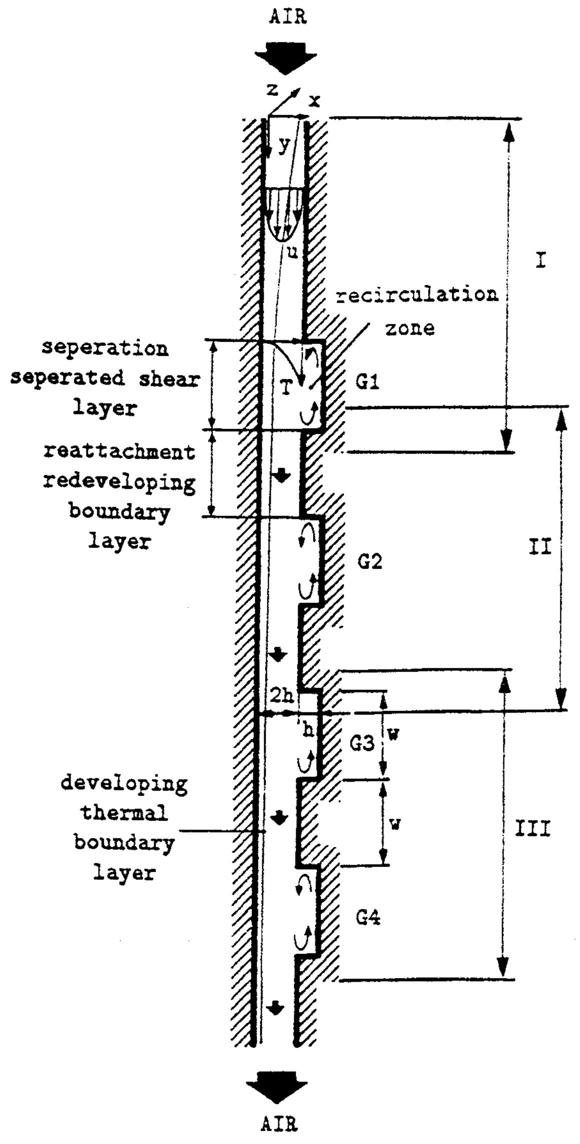

Figure 1. Schematic of the grooved geometry and the flow situation

present study and for possible future work. The simplest case, forced convection heat transfer between parallel plates heated symmetrically or asymmetrically, has been treated in the literature in detail: for example, Mercer et al. (1967) used interferometry to obtain heat transfer data in forced convection flow between parallel flat plates, and in the review publication of Shah & London (1978) the interested reader can find further references. Numerical solutions have been published by several authors: Bhatti & Aung (1984) obtained numerical results for a single groove, Durst et al. (1988) analysed channel flow over fences, Ghaddar et al. (1986) and Patera & Mikić (1986) obtained numerical solutions for fully developed flow conditions in a grooved channel — but less data is available for the developing flow situation. Aung's (1983) experimental work on heat transfer in a geometry with a single cavity has provided results and explanations of heat transfer for cavities with different aspect ratios, which is certainly of practical interest. In the work of Patera & Mikić (1986) and Ghaddar et al. (1986), numerical and experimental results for resonant heat transfer enhancement in the grooved geometry for fully developed flow conditions have been presented. Heat transfer on several roughness elements has also been analysed experimentally on a macro scale, for example by Ichimiya (1987). Although a lot of work on this topic has been published in the open literature, questions considering a systematic presentation of heat transfer data, which would enable the prediction of the system behaviour and optimization with respect to heat transfer augmentation and increased pressure drop — still remain open.

In practical applications, both the developing and the fully developed flow situation is of interest. This study analyses the physical situation where the flow is fully developed hydrodynamically, as presented schematically in figure 1. The development of the thermal boundary layer starts on the heated wall after the entry section. The boundary layer separates at the first groove, on its opening wall, and above the groove a separated shear layer is formed. Inside of the groove, a recirculation region exists. At the closing wall of the groove reattachment occurs, and on the wall behind the groove, the boundary layer redevelops until the opening wall of the second cavity has been reached. In the second and the following grooves, the situation described for the first one is repeated. Gradually, a thermally developed flow situation is reached, characterized by periodically repeating temperature fields (not analysed in this paper). In order to obtain detailed data on temperature fields without disturbing the flow, the experimental technique of holographic interferometry was chosen.

2. THE EXPERIMENTAL SETUP

The experimental setup used in this investigation is presented in figure 2. The test channel consists of the entry section (ENS), the test section itself (TS) and the exit section (EXS). The entry section is a 0.9 m long (47 times the hydraulic diameter), 0.22 m wide and 0.01 m high parallel plate duct, which provides fully developed flow conditions at the beginning of the test section. Air enters the channel, the direction of the flow indicated by arrows, through a curved entrance to reduce the effects of entrance drag. The walls of the test section are manufactured of aluminium (of a common block to avoid misalignment), and provided with water channels to keep the wall temperatures constant by constant temperature water baths (TH_H and TH_C). The grooved wall is heated to a temperature $T=T_H$, and the temperature of the cold wall is kept equal to the temperature of the air entering the test section ($T = T_{in} = T_C$). The cross section of the air flow area is 0.22 m wide (in the direction of the z

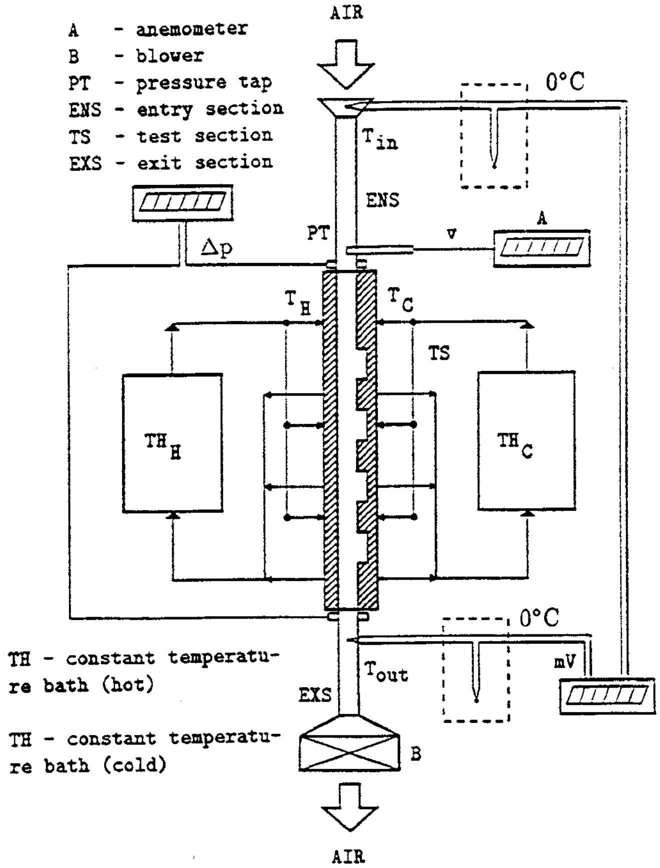

Figure 2. The experimental setup

axis), $2h = 0.01$ m high (x direction), and the depth of the grooves h is 0.005 m. The length of the test section is 0.22 m (y direction). The front and back sides of the test section are closed by glass windows which enable the transillumination of the heated region and the viewing of the measurement region. The exit section carrying the blower (B) is 0.3 m in length. Air flow is produced by the blower operating in suction mode, and flow velocity is varied by changing the dc supply voltage of the blower.

The temperature of the air entering the test section T_{in} was measured by a battery of five nickelchrom-constantan thermocouples connected in series and distributed along the cross sectional area — to provide average temperature values and yield amplified emf, and thus enhance measurement accuracy. Air flow velocity profile measurements were obtained by a schiltknecht hot wire anemometer thermo-air type 442. Pressure drop measurements Δp were taken with a pressure transducer Ziegler-Setra Series 239. Four pressure taps, 0.0001 m in diameter, are located in the flanges between entry and test section and also between test section and exit section. The pressure transducer was calibrated by a Betz manometer. Wall temperatures in the test section were monitored by 25 nickelchrom-constantan thermocouples integrated into the wall surface. For each measurement, temperature readings were taken by a Philips Multipoint Data Recorder MP 8237A. They served as reference values for interferometric measurements. Air outlet temperature T_{out} was measured by a battery of five nickelchrom-constantan thermocouples, similarly to the measurement of the inlet temperature.

3. THE EXPERIMENTAL METHOD

Measurements of the temperature fields in the test section were obtained by holographic interferometry, a method widely accepted in the study of transport processes (Hauf & Grigull (1970), Mayinger & Panknin (1974)) because of the unique advantages it offers: it does not influence the process to be examined. From the photographs, both qualitative and quantitative information on complete temperature fields can be extracted. The optical setup used for the interferometric measurements in this work, has been described in detail by Mayinger & Panknin (1974). In the measurements, an argon ionen laser with $\lambda = 514.5\ 10^{-9}$ m wavelength has been used. The optical method and the technique of the evaluation of interferometric images will not be elaborated here, as there is sufficient literature available treating this topic (Hauf & Grigull (1970), Vest (1979)).

The interferograms were recorded on photographic film by a camera, and the processed negative films were analysed and measured by a photometer. As the test section length (0.22 m) is greater than the diameter of the expanded laser beam (0.078 m), data on temperature fields along the test section were obtained by taking measurements in three different sections of the test channel (marked by I, II and III in figure 1) which partly overlapped each other. Typical average exposition times for recording the interferograms were in the range from 1/30 to 1/125 s.

4. RESULTS AND DISCUSSION

Heat transfer behaviour for the grooved geometry has been analysed for a set of operating parameters. Flow conditions were specified by the Reynolds number, de-

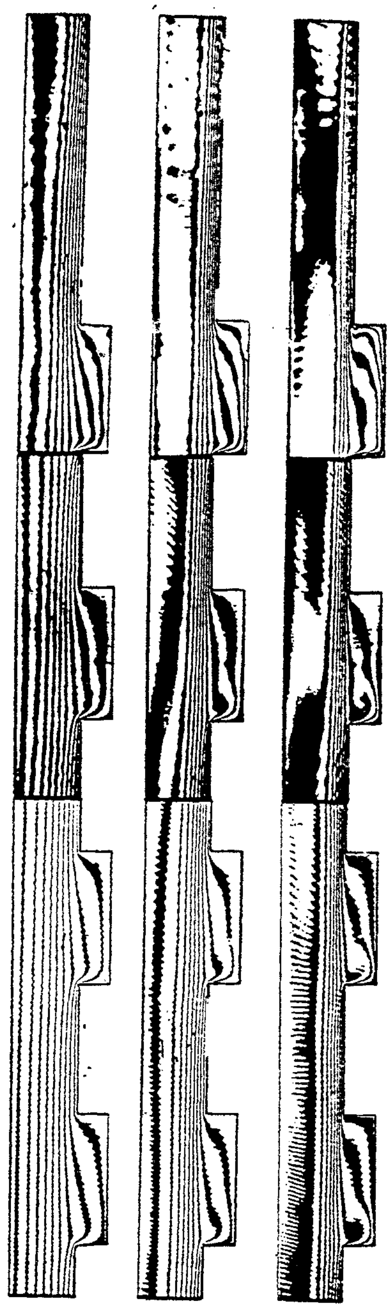

Figure 3. Interferogram sets for $\overline{\Delta T}$=30 K and Re=293, Re=604 and Re=1561, taken by infinite fringe field technique

fined through the hydraulic diameter D_h, Re = $v_m D_h$ / ν, where v_m is the mean flow velocity. The flow was fully developed. Thermal boundary conditions were defined by isothermal test section walls. Experimental runs were performed for Reynolds numbers in the range from Re = 290 to Re = 1600, so that laminar flow conditions were present. The aspect ratio of the channel (width : height = 22 : 1) was chosen in order to obtain essentially two dimensional flow conditions. The accuracy of the velocity measurements was 2%.

Interferograms were obtained both by the infinite

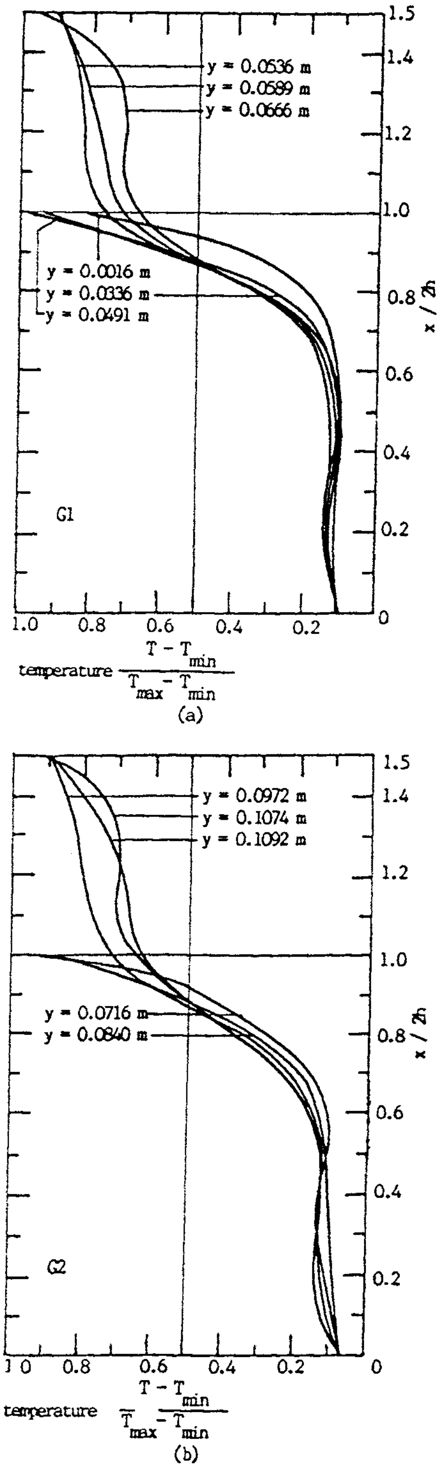

Figure 4.1. Temperature fields for $\overline{\Delta T}$=45 K and Re=1220.8 - (a) first groove, (b) second groove

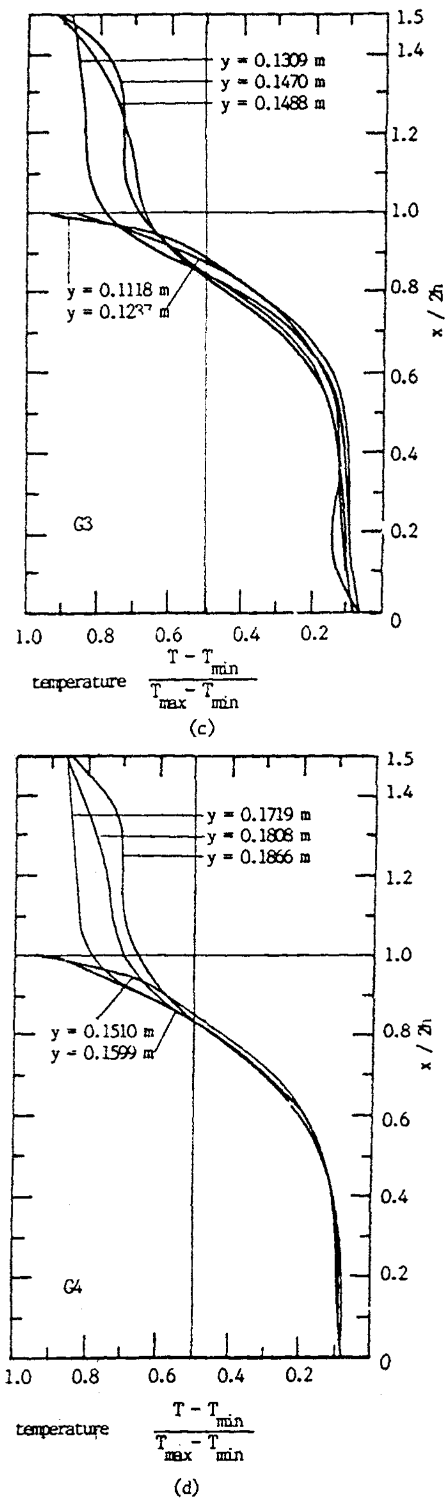

Figure 4.2. Temperature fields for $\overline{\Delta T}$=45 K and Re=1220.8 - (c) third groove, (d) fourth groove

fringe field and by the finite fringe field method, for each experimental run. Details about the evaluation technique and the measurement accuracy can be found in the work of Sterr (1989). Results obtained by both techniques were in excellent agreement. Also, temperature distributions obtained for the three sections of the test channel (I, II, III) showed very good agreement, as it can be seen in figure 3. The maximum deviation of the interferometric temperature measurements compared to values obtained by thermocouples was about 7%.

Photographs taken for different experimental runs showed the same basic behaviour, so that the selected three sets of interferograms in figure 3, are representative for the thermal behaviour of the system. Qualitatively, nite fringe field technique, agree very well with the results of the numerical simulation presented by Ghaddar et al. (1986) and Patera & Mikić (1986), for the fully developed flow situation. In figure 3, two heat transfer regions can be distinguished. In the groove region, the temperature field is affected by the recirculating flow, but the groove vortex does not significantly influence the channel part of the flow and the heat transfer in the channel domain.

In figure 4, temperature profiles for Re = 1220.8 and $\overline{\Delta T}$ = 45 K are presented. In the groove region, temperature profiles have a typical S shape. In the channel region, temperature profiles are of similar character along the test section, and they show similar behaviour in the corresponding sections of the groove. It is clear, that the temperature drop in the channel part is much greater than the temperature drop inside the groove (also shown in figure 5), so that the first one governs the heat transfer. The main temperature drop (approximately 80%) occurs in the vicinity of the wall, in the region from x/2h = 0.6 to x/2h = 1.0. A gradual decrease of the temperature gradient $\Delta T/\Delta x$ can be observed along the test section in the y direction. Inside the groove, immediately after the opening wall, the temperature gradient on the wall is extremely small. With increasing y, the gradient increases, reaches a maximum in the last quarter section of the groove, and afterwards it starts decreasing towards the closing wall. In figure 4a, the curve for y = 0.666 m corresponds to the maximum of the temperature gradient. In figure 4b, the temperature profile for y = 0.1092 m corresponds to the cross section after this maximum value has been reached. The differences between the temperature profiles in the channel region decrease with increasing groove number, towards the thermally fully developed region.

In figure 5, Nusselt number values Nu(y) are presented. The local Nusselt number is calculated as Nu(y) = $D_h\ (dT/dx)_w\ /\ (T_w - T_\infty)$ where $(dt/dx)_w$ is the temperature gradient at the wall, and T_∞ is a reference temperature. The Nusselt number values decrease gradually as the thermal boundary layer develops. Immediately after the opening wall of the first groove, the Nusselt number value falls abruptly to approximately 17% of the attached flow value. Then it increases slowly along the cavity, to reach, abruptly again, a peak value in the last quarter section of the groove. The peak value is smaller than the attached flow value. After this peak, the Nusselt number value falls again towards the closing wall of the first groove. Immediately after reattachment, in the beginning redevelopment region, Nu(y) is very high — three times the corresponding attached flow value — after which it decreases continuously until the separation point. In the second groove, the behaviour described for the first groove repeats. In the redevelopment region after the second groove, a new maximum is reached, a multiple of the corresponding attached flow value, but significantly lower than the one after the first groove. In the grooves, peak Nu(y) values become smaller, and the rise towards

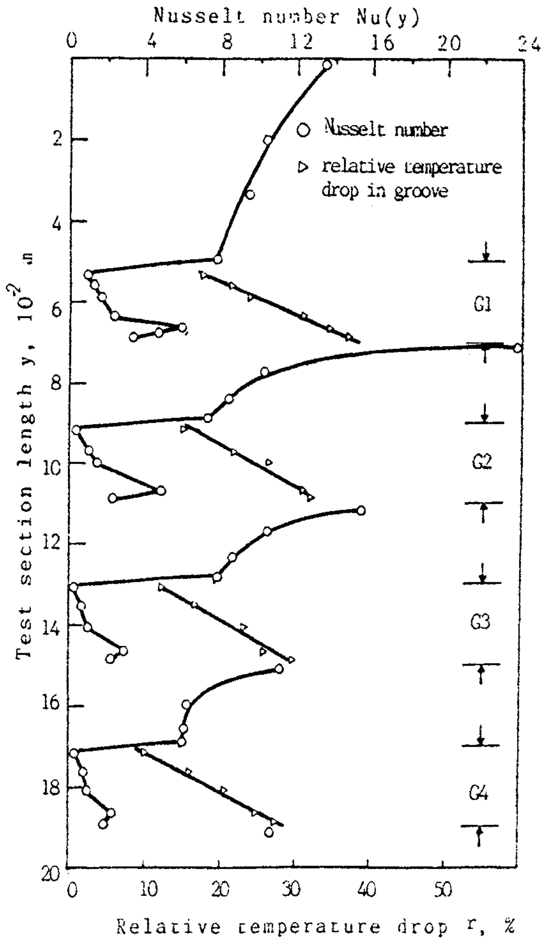

Figure 5. Local Nusselt number and relative temperature drop inside the groove compared to total temperature drop vs. y for $\overline{\Delta T}$=45 K and Re=1220.8

the maximum is less abrupt with increasing groove number. Also, absolute values decrease gradually towards the value in thermally fully developed flow. It is obvious that heat transfer augmentation in this geometry is due to the strong increase of heat transfer in the redevelopment region. In figure 5, the relative temperature drop inside the groove, compared to the total temperature drop across the channel, is presented. The relative temperature drop shows a linear increase along the groove — starting with 17% and ending with 36% for the first groove. This linear dependence remains for the following grooves, with slightly decreasing absolute values. Pressure drop measurements vs. Reynolds number in the test section, are presented in figure 6. In the same figure, typical measurement data for the relative temperature change from air inlet to air outlet vs. Reynolds number is shown, for $\overline{\Delta T}$ = 45 K. Other experimental runs show similar character.

5. CONCLUSIONS

The aim of this work was to point out some aspects

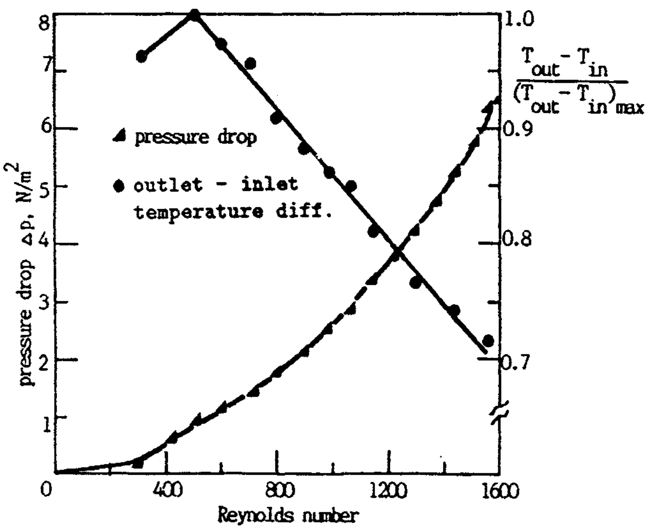

Figure 6. Pressure drop and temperature increase in test section vs. Reynolds number

of heat transfer in laminar forced convection channel flow in a grooved geometry with a developing thermal boundary layer. The experimental results indicate the following: (i) The temperature profiles in the region of the grooves show a specific S shape. In the channel part of the flow they are essentially uninfluenced by the recirculating zone in the groove. (ii) The significant share of temperature drop belongs to the channel region. (iii) Augmentation of heat transfer is due to the high heat transfer in the redevelopment zone after the grooves. (iv) Temperature fields and Nusselt number values tend to reach values characteristic for the thermally fully developed situation.

Further work could be directed towards obtaining theoretical solutions and sufficient experimental data to enable the prediction of the system behaviour. Flow visualization and velocity field measurements would contribute to the better understanding of the physical phenomena in this complex geometry. The analysis of different groove aspect ratios would certainly be of practical interest, and the possibility to use the effects of resonant heat transfer enhancement, is an interesting topic for future research.

6. ACKNOWLEDGEMENTS

The experiments presented in this paper were carried out under the auspices of Lehrstuhl A für Thermodynamik, TU München. The support is gratefully acknowledged.

7. REFERENCES

Aung, W., 1983, An Interferometric Investigation of Separated Forced Convection in Laminar Flow Past Cavities, ASME J. Heat Transfer, Vol. 105, pp. 505-512.

Bhatti, A., & Aung, W., 1984, Finite Difference Analysis of Laminar Separated Forced Convection in Cavities, ASME J. Heat Transfer, Vol. 106, pp. 49-54.

Durst, F., Founti, M. & Obi, S., 1988, Experimental and Computational Investigation of the Two-Dimensional Channel Flow Over Two Fences in Tandem, ASME J. Heat Transfer, Vol. 110, pp. 48-54.

Ghaddar, N. K., Korczak, K. Z., Mikić, B. B. & Patera, A. T., 1986, Numerical Investigation of Incompressible Flow in Grooved Channels. Part 1. Stability and Self-sustained Oscillations, J. Fluid Mech., Vol. 163, pp. 99-127.

Ghaddar, N. K., Magen, M., Mikić, B. B. & Patera, A. T., 1986, Numerical Investigation of Incompressible Flow in Grooved Channels. Part 2. Resonance and Oscillatory Heat Transfer Enhancement, J. Fluid Mech., Vol. 168, pp. 541-567.

Hauf, W. & Grigull, U., 1970, Optical Methods in Heat Transfer, in Advances in Heat Transfer, Vol. 6, pp. 133-366, Academic Press Inc., New York.

Ichimiya, K., 1987, Effects of Several Roughness Elements on an Insulated Wall for Heat Transfer from the Opposite Smooth Heated Surface in a Parallel Plate Duct, ASME J. Heat Transfer, Vol. 109, pp. 68-73.

Mayinger, F., & Panknin, W., 1974, Holography in Heat and Mass Transfer, Proc. 5th Int. Heat Transfer Conf., Tokyo, Vol. 6, pp. 28-43.

Mercer, W. E., Pearce, W. M., & Hitchcock, J. E., 1967, Laminar Forced Convection in the Entrance Region Between Parallel Flat Plates, ASME J. Heat Transfer, Aug. 1967, pp. 251-257.

Patera, A. T. & Mikić, B. B., 1986, Exploiting Hydrodynamic Instabilities. Resonant Heat Transfer Enhancement, Int. J. Heat Mass Transfer, Vol 29, No. 8, pp. 1127-1138.

Shah, R. K. & London, A. L., 1978, Laminar Flow Forced Convection in Ducts, in Advances in Heat Transfer, Suppl. 1, Academic Press, New York.

Sterr, S., 1989, Diplomarbeit, Lehrstuhl A für Thermodynamik, TU München.

Vest, C. M., 1979, Holographic Interferometry, John Wiley & Sons, New York.